Effective Medium Theory of Magnetization Reversal in Magnetically Interacting Particles

Heliang Qu and JiangYu Li

***Abstract*—We report an effective medium theory of magnetization reversal and hysteresis in magnetically interacting particles, where the intergranular magnetostatic interaction is accounted for by an effective medium approximation. We introduce two dimensionless parameters, λ and h_0, that completely characterize the hysteresis in a ferromagnetic polycrystal when the grain size is much larger than the exchange length so that the exchange coupling can be ignored. The competition between the anisotropy energy and the intergranular magnetostatic energy is measured by λ, while the competition between the anisotropy energy and Zeeman's energy is measured by h_0. The hysteresis loop, magnetostatic energy density, and anisotropy energy density calculated by using this theory agrees well with micromagnetic simulations. The calculations also reveal that the subnucleation field switching due to the magnetic field fluctuation is important when the magnet is not very hard, and that has been accounted for by a probability-based switching model.**

***Index Terms*—Effective medium approximation, hysteresis, intergranular magnetostatic interaction, magnetization reversal.**

I. Introduction

STONER and Wohlfarth's celebrated model [1] has been widely used for more than 50 years to analyze the magnetization reversal in polycrystalline permanent magnets. The underlying assumption of the Stoner–Wohlfarth model is that each grain in the polycrystal reverses its magnetization through rotation without interacting with each other, and as a result, the remanent magnetization is simply given by the volume average of magnetization over the polycrystal

$$M_r = M_s \langle \cos\theta \rangle \tag{1}$$

where M_s is saturation magnetization and θ is the angle between the remanent magnetization of the polycrystal and the easy axis of the grain. While the model provides an accurate estimate of the remanence of most permanent magnets, it also highlights the importance of intergranular magnetic interactions in the design and optimization of new magnetic materials. Permanent magnets with large remanence and coercivity are desirable for energy storage due to their high energy product [2], and in order to enhance the energy product of polycrystalline magnets, the intergranular magnetic interactions must be strengthened, so that higher remanence than Stoner–Wohlfarth's prediction can be accomplished.

Manuscript received February 3, 2004; revised November 20, 2004. This work was supported by the Nebraska Research Initiative.

The authors are with the Department of Engineering Mechanics, University of Nebraska-Lincoln, Lincoln, NE 68588-0526 USA (e-mail: ahqu@hotmail.com; jiangyuli@unlnotes.unl.edu).

Digital Object Identifier 10.1109/TMAG.2004.843318

One of the breakthroughs was made about ten years ago when an exchange coupling mechanism was proposed to enhance the energy product of permanent magnets [3]. The idea is to mix the magnetic hard and soft phases at nanoscale so that they can be coupled through the intergranular exchange interaction, leading to dramatically enhanced remanence and energy product. This again highlights the importance of intergranular magnetic interactions, and calls for new models that can take those interactions into account. While micromagnetic simulations are able to explain the remanence enhancement in exchange-spring magnets [4], they are often computationally extensive and time-consuming. There are also earlier efforts to modify the Stoner–Wohlfarth model by Atherton and Beattie using a mean field correction [5], where a magnetic field proportional to the average magnetization is introduced on top of the applied field to account for the magnetic interactions among grains, although they have not sought to determine the proportional parameter introduced for the correction in the modified model. We hope to address these issues here by developing an effective medium theory to analyze the magnetization reversal in magnetically interacting particles. Our preliminary results on remanence enhancement in polycrystalline magnets have been reported in [6], and in this paper magnetization reversal and hysteresis loops will be analyzed. We will focus on the magnetization reversal through coherent rotation only, and thus will not consider motions and pinnings of domain walls [7].

II. Energetics and Effective Medium Theory

We consider an assemblage of single-phase single-domain magnetic particles, with particle size smaller than the single domain limit so that no domain wall movement is involved, yet large enough compared to the exchange length so that the short-range exchange coupling can be ignored. As a result, the potential energy of the assemblage is given by

$$F = \int_{\Omega} \left(K_1 \sin^2 \alpha[\theta] - \mathbf{J} \cdot \mathbf{H}_0 - \frac{1}{2} \mathbf{J} \cdot \mathbf{H}_d \right) d\mathbf{x} \tag{2}$$

where the first term is the uniaxial anisotropy energy at the lowest order, with α being the angle between the local magnetic polarization $\mathbf{J}$ and the easy axis of the particles; the second term is Zeeman's energy, where $\mathbf{H}_0$ is the applied magnetic field; and the third term is the magnetostatic energy, where $\mathbf{H}_d$ is the demagnetizing field induced by the distribution of $\mathbf{J}$ in Ω, the region occupied by the assemblage. Here, $\alpha[\theta]$ is a function of θ which we seek to characterize at different $\mathbf{H}_0$, while θ is used to label different grains at different orientations. The configuration in a typical grain at orientation θ is schematically shown in Fig. 1.

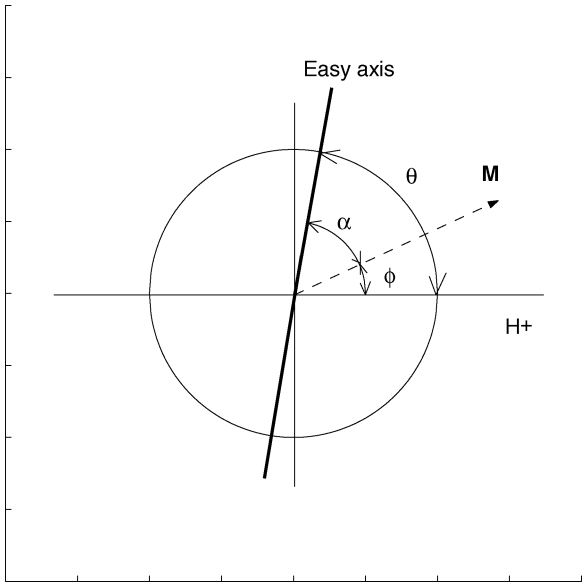

Fig. 1. The configuration for a grain at orientation θ.

We consider the long-range magnetostatic energy first. In micromagnetic simulation, calculating the magnetostatic energy often takes most of the CPU time due to its nonlocality. We intend to address this problem using an effective medium approximation which is believed to be accurate and computationally efficient. To this end, we decompose the magnetic polarization and magnetostatic field into two parts, and rewrite the magnetostatic energy as

$$F_d = -\frac{1}{2}\int_{\Omega} (\bar{\mathbf{J}} + \mathbf{J}') \cdot \left(\bar{\mathbf{H}}_d + \mathbf{H}'_d\right) d\mathbf{x} \tag{3}$$

where the overhead bar is used to represent the volume averaged quantities, and the primed ones are variations from the averages. Clearly, the cross products vanish because the volume integrations of primed field variables are zero. Notice that we have

$$|\bar{\mathbf{J}}| = J_h = fJ_s \tag{4}$$

where J_h is the magnitude of the macroscopic magnetic polarization along the applied field direction, J_s is the saturation magnetic polarization, and f is a dimensionless parameter introduced to represent the macroscopic magnetization in the polycrystal. In addition

$$\bar{\mathbf{H}}_d = -\frac{1}{\mu_0}\mathbf{N}_{\Omega}\bar{\mathbf{J}} \tag{5}$$

is the magnetic field induced by a uniform magnetic polarization $\bar{\mathbf{J}}$ in Ω, where $\mathbf{N}_{\Omega}$ is the demagnetizing factor depending on the shape of Ω. For in-plane magnetization in an ellipsoidal Ω with dimensions $a_1, a_2 \gg a_3$, $\bar{\mathbf{H}}_d$ is small.

The magnetic field induced by the magnetostatic interaction among particles,$\mathbf{H}'_d$, can be determined by solving Maxwell's equation

$$\nabla \cdot (\mu_0 \mathbf{H}'_d + \mathbf{J}') = 0 \tag{6}$$

for given distribution of $\mathbf{J}'$ using Green's function method [8]

$$\mathbf{H}'_d(\mathbf{x}) = -\frac{1}{\mu_0}\nabla \int_{\Omega} \nabla' g(\mathbf{x}, \mathbf{x}') \cdot \mathbf{J}'(\mathbf{x}') d\mathbf{x}' \tag{7}$$

where $g(\mathbf{x}, \mathbf{x}')$ is the magnetic Green's function, and ∇' denotes the gradient with respect to $\mathbf{x}'$. To carry out the analysis further, we recall that the grain size of the polycrystal is smaller than the single domain limit, and thus the magnetic polarization in individual grain is uniform. In addition, we assume that grains with identical orientation will have identical magnetic polarization, an *effective medium approximation*, so that

$$\mathbf{J}'(\mathbf{x}) = \sum_{k=1}^{n} \chi_k(\mathbf{x}) \mathbf{J}'_k \tag{8}$$

where n is the number of different orientations and

$$\chi_i(\mathbf{x}) = \begin{cases} 1, & \mathbf{x} \in \Omega_i \\ 0, & \text{otherwise} \end{cases} \tag{9}$$

is the characteristic function of a region Ω_i containing all grains having orientation i, in which magnetic polarization $\mathbf{J}'_i$ is uniform. Multiplying (7) by $\chi_i(x)$ leads to

$$\chi_i \mathbf{H}'_d = -\frac{1}{\mu_0}\sum_{k=1}^{n} \int_{\Omega} \chi_{ik}(\mathbf{x}, \mathbf{x}') \nabla \left[\nabla' g(\mathbf{x}, \mathbf{x}') \cdot \mathbf{J}'_k\right] d\mathbf{x}' \tag{10}$$

where $\chi_{ik}(\mathbf{x}, \mathbf{x}') = \chi_i(\mathbf{x})\chi_k(\mathbf{x}')$ is the two-point correlation function of grain distribution in the polycrystal, which gives the probability of locating grain orientation i at $\mathbf{x}$ and grain orientation k at $\mathbf{x}'$ simultaneously. When the two-point correlation function is ellipsoidal [9], we have

$$\begin{aligned} \chi_i \mathbf{H}'_d &= -\frac{1}{\mu_0}\sum_{k=1}^{n} \chi_{ik}(\mathbf{0}) \mathbf{N}_g \mathbf{J}'_k = -\frac{1}{\mu_0}\sum_{k=1}^{n} c_k \delta_{ik} \mathbf{N}_g \mathbf{J}'_k \\ &= -\frac{1}{\mu_0} c_i \mathbf{N}_g \mathbf{J}'_i \end{aligned} \tag{11}$$

with

$$\mathbf{N}_g = \int_{|\mathbf{y}|<1} \nabla \left(\nabla' g(\mathbf{x}, \mathbf{x}')\right) d\mathbf{x}' \tag{12}$$

where $y_i = (x_i - x'_i)/a_i$ while a_i is the dimension of principal axis of the ellipsoid, and $c_i = \langle \chi_i(\mathbf{x}) \rangle$ is the volume fraction of grain i or the probability of locating grain i at $\mathbf{x}$. In fact, $\mathbf{N}_g$ is a second rank tensor that can be regarded as the demagnetizing factor of grains depending on their shape. Integrating (11) over the polycrystal Ω, we obtain

$$\mathbf{H}'_d = -\frac{1}{\mu_0}\mathbf{N}_g \mathbf{J}' = -\frac{1}{\mu_0}\mathbf{N}_g(\mathbf{J} - \bar{\mathbf{J}}) \tag{13}$$

which is the intergranular magnetostatic field we try to characterize. For spherical distribution, $\mathbf{N}_g = (1/3)\mathbf{I}$, which leads to

$$F_d = \frac{V}{6\mu_0}\left(J_s^2 - J_h^2 + 3N_{\Omega} J_h^2\right) \tag{14}$$

where V is the volume of Ω, and N_Ω is the in-plane demagnetizing factor. Even though N_Ω is small for thin-plate magnets, it cannot be ignored for nonhard magnetic materials. The treatment for more general grain shape is straightforward. Notice that the first term of the magnetostatic energy is a constant and thus is irrelevant in the following energy minimization and will be ignored. It is emphasized that we have derived the interaction field analytically using the effective medium approximation, while in Atherton and Bettie [5] this interaction field is introduced phenomenologically.

The total anisotropy energy of the system can be determined as

$$F_a = VK_1 \left\langle \sin^2 \alpha[\theta] \right\rangle \tag{15}$$

and Zeeman's energy can be evaluated as

$$F_z = -V\mathbf{H}_0 \cdot \bar{\mathbf{J}} = -VH_0 J_s f. \tag{16}$$

By combining all these energy contributions we obtain the following energy density of the assemblage:

$$F = K_1 \left\langle \sin^2 \alpha[\theta] \right\rangle - H_0 J_s f - \frac{J_s^2}{6\mu_0} f^2 (1 - 3N_\Omega) \tag{17}$$

which can be rewritten as

$$\begin{aligned} F &= K_1 \left\{ \left\langle \sin^2 (\phi[\theta] - \theta) \right\rangle - h_0 f - \lambda f^2 (1 - 3N_\Omega) \right\} \\ &= K_1 \left(\left\langle \sin^2 (\phi[\theta] - \theta) \right\rangle - h_0 f - \lambda^* f^2 \right) \end{aligned} \tag{18}$$

where ϕ is the angle between the magnetization and the applied field direction (see Fig. 1)

$$\alpha = \phi - \theta \tag{19}$$

and we have introduced two dimensionless parameters

$$\lambda = \frac{J_s^2}{6K_1\mu_0}, \quad h_0 = \frac{H_0 J_s}{K_1} \tag{20}$$

with λ characterizing the competition between anisotropy energy and intergranular magnetostatic energy, while h_0 characterizing the competition between anisotropy energy and Zeeman's energy. We have also used

$$\lambda^* = \lambda(1 - 3N_\Omega) \tag{21}$$

to correct the influence of demagnetization due to the shape of the specimen. Notice that the hard phase has a small λ while the soft phase has a large λ. For example, in an exchange-spring magnet consisting of $Fe_{14}Nd_2B$ and $\alpha-$Fe, λ is approximately 0.1 and 10 for the hard and soft phase, calculated using data from [10]. As a result, in hard phase, the intergranular magnetostatic interactions can be ignored, and our theory should recover to the classical Stoner–Wohlfarth model. When a softer phase is involved, however, this interaction can no longer be neglected.

III. Magnetization Reversal and Hysteresis

A. Equilibrium and Stability

Now we seek to determine $\phi[\theta]$ at every applied magnetic field H_0 or h_0, so that the magnetic hysteresis loop can be derived. To be specific, we assume that the easy axes of grains are constrained within $x_1 - x_2$ plane for simplicity in the following analysis, although the theory can be applied to three-dimensional texture without difficulty. With such assumption, the orientational averaging in the polycrystal can be carried out as

$$\left\langle \sin^2 \alpha[\theta] \right\rangle = \int_0^\pi \sin^2 \alpha[\theta] w(\theta) d\theta \tag{22}$$

and

$$f = \int_0^\pi \cos \phi[\theta] w(\theta) d\theta \tag{23}$$

where $w(\theta)$ is the orientation distribution function (ODF) that describes the probability of locating a grain at a particular orientation, which can be an arbitrary function of θ [11], [12].

We propose that under any applied magnetic field, the magnetization distribution in the polycrystal, $\phi[\theta]$, will minimize the potential energy of the system, such that

$$\frac{\delta F}{\delta \phi} = 0 \tag{24}$$

resulting in

$$\int_0^\pi [2 \sin\alpha \cos\alpha + h_0 \sin\phi + 2\lambda^* f \sin\phi] w(\theta) \delta\phi(\theta) d\theta = 0 \tag{25}$$

which leads to the following equation of ϕ at every θ

$$\sin 2(\phi - \theta) + (2\lambda^* f + h_0) \sin\phi = 0. \tag{26}$$

It is clear that (26) and (23) are coupled together: the effective magnetization f depends on the magnetization distribution ϕ, whose determination in turn requires the knowledge of f. As a result, they need to be solved numerically by iteration in general with the material property λ, specimen geometry N_Ω, and the applied field h_0 given. It is worthwhile to point out that (26) typically has two or four solutions depending on λ^* and h_0, and one or two of them would be unstable. When there are two stable solutions, the one that is actually adopted at an applied magnetic field depends on the history of the applied field, which leads to possible metastable state and hysteresis. When a grain is in metastable state, the energy at the third unstable solution gives the energy barrier to the equilibrium state of absolute energy minimum.

In order to determine the stability of a solution, we resort to the second variation of energy functional F with respect to ϕ, which leads to

$$\frac{\delta^2 F}{\delta \phi^2} = K_1 \left[\frac{\delta^2 k}{\delta \phi^2} - 2\lambda^* \left(\frac{\delta f}{\delta \phi} \right) g - 2\lambda^* f \left(\frac{\delta g}{\delta \phi} \right) - h_0 \frac{\delta g}{\delta \phi} \right] \tag{27}$$

where we have used the following notations:

$$k = \int_0^\pi \sin^2 (\phi[\theta] - \theta) w(\theta) d\theta \tag{28}$$

$$g = \frac{\delta f}{\delta \phi} = -\int_0^\pi \sin \phi[\theta] w(\theta) d\theta \tag{29}$$

and

$$\frac{\delta^2 f}{\delta\phi^2} = \frac{\delta g}{\delta\phi} = -f = -\int_0^\pi \cos\phi[\theta] w(\theta) d\theta. \tag{30}$$

Expanding (27), we have

$$\frac{\delta^2 F}{\delta\phi^2} = 2K_1 \int_0^\pi \left[\cos 2\alpha + \lambda^* g \sin\phi + \lambda^* f \cos\phi + \frac{h_0}{2}\cos\phi\right] \cdot w(\theta)\delta^2\phi(\theta) d\theta \tag{31}$$

As a result, the stability of the solution at each θ can be determined by

$$\gamma = \cos 2(\phi - \theta) + \lambda^* g \sin\phi + \left(\lambda^* f + \frac{h_0}{2}\right)\cos\phi \tag{32}$$

with $\gamma > 0$ indicating a stable solution and $\gamma < 0$ indicating an unstable solution and possible reversal of magnetization.

B. Hysteresis and Energy Density

Equations (26), (23), and (32) allow us to determine the macroscopic magnetization at every applied magnetic field, and as a result, the magnetic hysteresis loop can be derived. In particular, let us assume that at a positive h_0 the magnetization distribution is $\phi[\theta]$, one of the stable solutions at θ. Then let h_0 be reduced and reversed to opposite direction. Sooner or later, the current ϕ at a particular θ will become unstable due to the increasing negativeness of h_0, which will reach the nucleation field and result in magnetization reversal. When the magnetization at all θ is reversed, the macroscopic magnetization reversal of the polycrystal is completed. Thus, we have a model that will allow us to calculate the magnetization reversal and hysteresis loop from physical mechanism without using any fitting parameters. One of the key observations here is that the magnetic hysteresis of a material is completely characterized by two dimensionless parameters λ (or λ^*) and h_0. In other words, magnets with different K_1 and J_s but identical λ^* and $w(\theta)$ will have identical hysteresis loops plotted on dimensionless scales as f versus h_0, although they will be different if plotted as J_h versus H_0. This will be demonstrated in our following discussions. We also want to point out that the current theory uses energy minimization to derive the hysteresis loop, and thus is limited to quasi-static loading condition and further modification is necessary before it can be applied to study the dynamic process of magnetization reversal.

We have implemented our model in a C code, where Gaussian quadrature method is adopted for numerical integration in (23) with given ϕ and bisecting method is used to solve (26) for given f [13]. At any given applied field, the solution from the previous step is taken as an initial guess, and the iteration continues until the convergence criterion is satisfied. To validate the model, we compared our calculation with the simulation results obtained using micromagnetic code Object Oriented MicroMagnetic Framework (OOMMF) developed at the National Institute of Standards and Technology [14]. The simulations were conducted on ellipsoidal samples with dimensions $a_1 = a_2 = 300$ nm and $a_3 = 10$ nm, which were divided into cubic cells of 10 nm long. For this geometry, the demagnetizing factor $N_\Omega = 0.0502$. Two-dimensional random distribution of easy axes was assumed among all the cells, with magnetization within each cell assumed to be uniform, although more general orientation distribution can be treated in our model. To derive the major hysteresis loop, the samples were saturated by applying a sufficient large magnetic field along the x_1 direction with the initial distribution of magnetization assumed to be random. The magnetic field is then reduced gradually step by step, reversed, and then saturated in the opposite direction. To derive the minor hysteresis loop, we reverse the applied magnetic field before saturation. In all the simulations, the exchange constant was assumed to be zero to allow the comparison with our model, and the damping coefficient was taken to be 0.5. All the calculations were carried on a Pentium IV-based desktop computer. In all the following figures, *simulated results* refer to results from OOMMF simulation, while *calculated results* refer to results from our effective medium model.

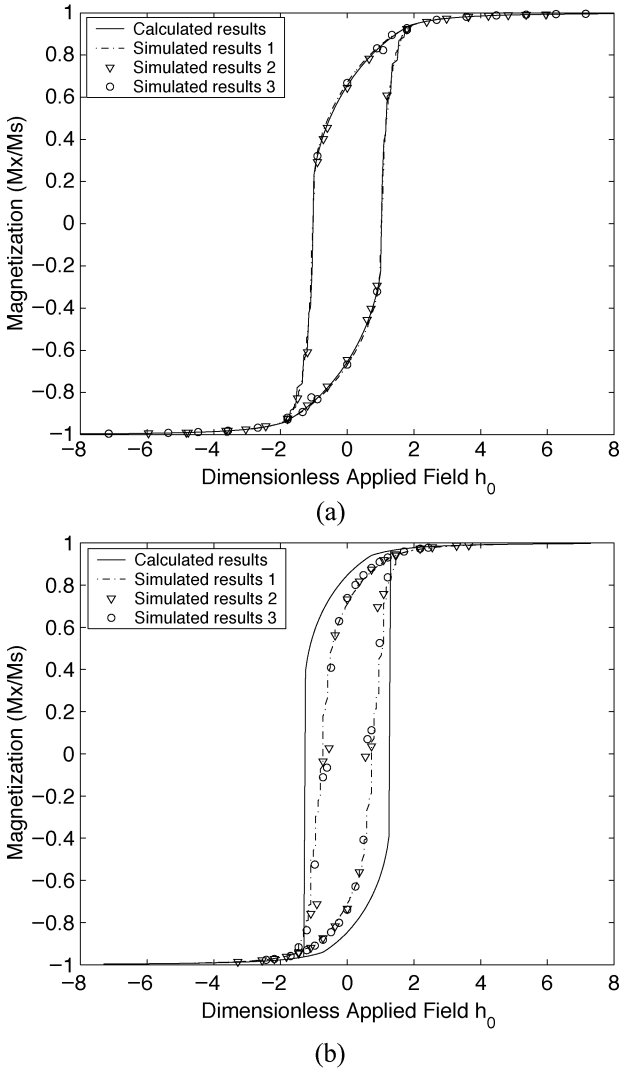

Fig. 2. Dimensionless magnetic hysteresis loop f versus h_0 calculated from effective medium theory and micromagnetic simulation: (a) $\lambda = 0.08$; (b) $\lambda = 0.8$.

We first present the calculated hysteresis loops of hard magnets ($\lambda = 0.08$) and intermediate magnets ($\lambda = 0.8$) compared with micromagnetic simulations, as shown in Fig. 2. For each

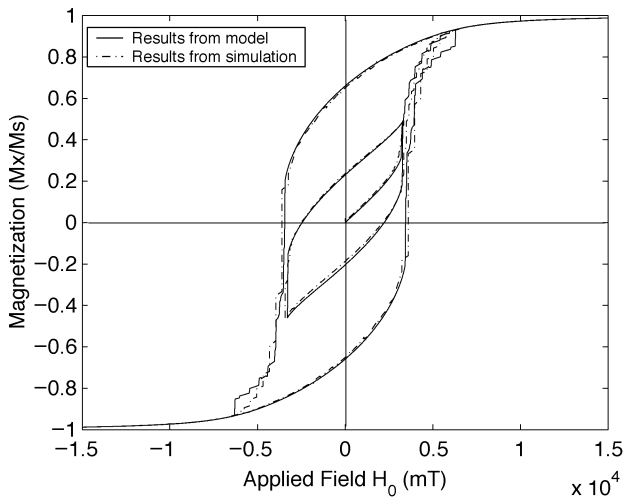

Fig. 3. Minor loops of $Fe_{14}Nd_2B$ obtained using the effective medium calculation and OOMMF simulation.

λ, three different combinations of K_1 and J_s are used in micromagnetic simulations, with K_1 differing by a factor of 1, 4, and 9 and J_s differing by a factor of 1, 2, and 3, respectively. Despite the large difference in K_1 and J_s, the three hysteresis loops obtained from micromagnetic simulations for both λ collapse into a single loop if plotted on dimensionless scales as f versus h_0, as we predicted from our theory. In addition to the calculation of major hysteresis loop, the proposed model is also capable of calculating the virgin curve and minor hysteresis loop, as shown in Fig. 3 for $Fe_{14}Nd_2B$ plotted on a dimensional scale; the agreement between effective medium calculation and micromagnetic simulation for the virgin curve and minor loop is excellent. As a matter of fact, we are able to calculate the magnetization curve under an arbitrary loading history.

We also notice that for the hard magnet, our calculation is nearly identical to the micromagnetic simulation, while for the intermediate one, the agreement is good, but the model overestimates both remanence and coercive field. We believe this is due to the magnetization reversal under subnucleation field [15] because of the fluctuation of magnetic field within the polycrystal. In other words, the less impressive comparison between our model and micromagnetic simulation is because we have not yet accounted for the magnetization distribution accurately due to the switching under subnucleation field, not because our effective medium approximation for the intergranular magnetostatic interactions is inaccurate. In fact, if the magnetization distribution is known, our effective medium calculation is able to calculate the magnetostatic energy accurately, as we will show. Since we have not taken into account subnucleation field switching, we overestimated the remanence, resulting in an overestimated coercive field.

In order to support our claim, we plotted the magnetostatic energy density as a function of the applied magnetic field h_0 for a hard magnet ($\lambda = 0.08$) and an intermediate magnet ($\lambda = 0.5$), as shown in Fig. 4, calculated from both our effective medium theory and micromagnetic simulations. In both cases, the magnetostatic energy is small near saturation, where the magnetization distribution is uniform and the intergranular magnetostatic energy is zero, and the demagnetization of the specimen is the only source of the magnetostatic energy. Near

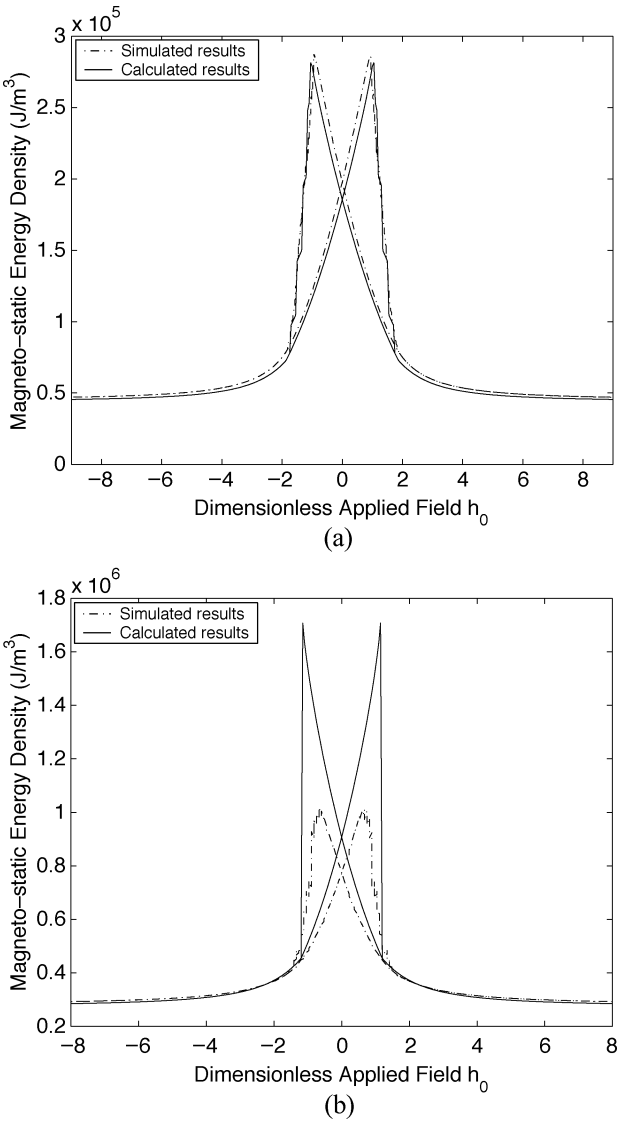

Fig. 4. Magnetostatic energy density as a function of the applied magnetic field h_0 calculated from effective medium theory and micromagnetic simulation: (a) $\lambda = 0.08$; (b) $\lambda = 0.5$.

the coercive field, the intergranular magnetostatic interaction increases due to the nonuniform magnetization distribution, resulting in higher magnetostatic energy. The effective medium theory agrees very well with micromagnetic simulation for hard magnet, while for the intermediate magnet, the agreement is less impressive, especially when the applied magnetic field is close to the coercive field. In hard magnets, the energy barrier for magnetization reversal is high and subnucleation field switching is rare, and we are able to characterize the magnetization distribution accurately under any applied magnetic field because of that. As a result, the magnetostatic energy calculated from the effective medium theory agrees with micromagnetic simulation very well, suggesting that it is indeed a good and efficient approximation. In intermediate magnets, however, the energy barrier is smaller, and the probability of subnucleation field switching is higher, and as a result, the magnetostatic energy calculated from the effective medium theory does not agree as well with the micromagnetic simulation. This is not because of the failure of the effective medium approximation, but because

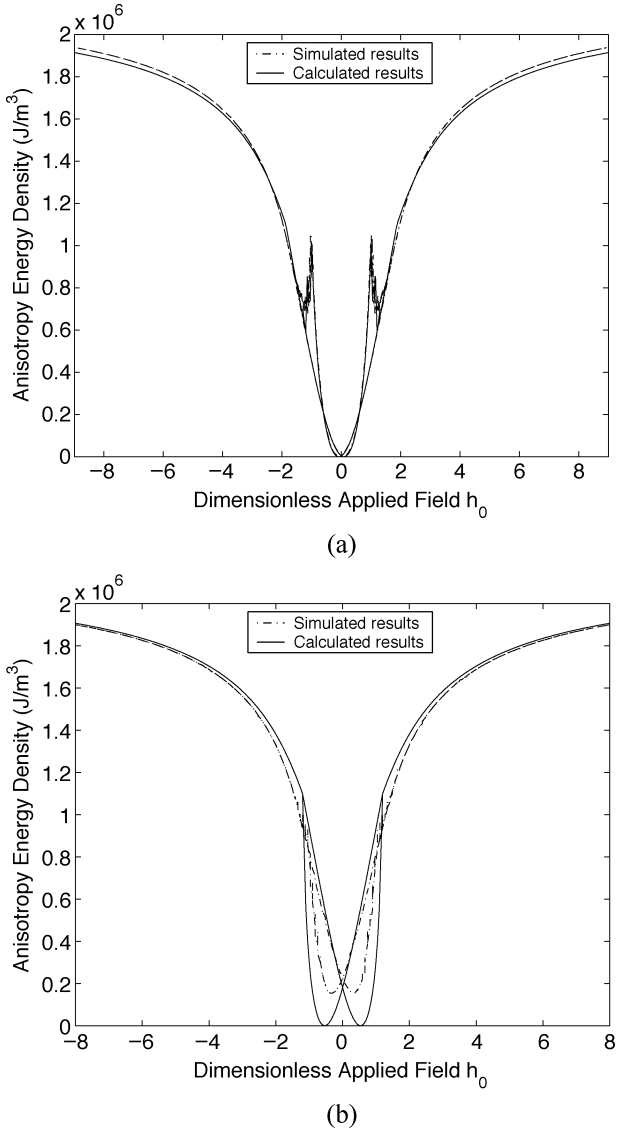

Fig. 5. Anisotropy energy density as a function of the applied magnetic field h_0 calculated from effective medium theory and micromagnetic simulation: (a) $\lambda = 0.08$; (b) $\lambda = 0.5$.

we are unable to characterize the magnetization distribution accurately without addressing the subnucleation field switching, especially when the applied field is close to the coercive field. This again suggests that our effective medium approximation for the intergranular magnetostatic interaction is accurate, and magnetic field fluctuation must be considered to take into account of the subnucleation field switching, so that magnetization distribution in nonhard magnets can be accurately characterized; we will address that in the next section.

Our argument can also be inferred from the anisotropy energy density plotted as a function of the applied field h_0 for a hard magnet ($\lambda = 0.08$) and an intermediate magnet ($\lambda = 0.5$), as shown in Fig. 5, calculated from both effective medium theory and micromagnetic simulations. In both magnets, the anisotropy energy near saturation is high because of a uniform magnetization distribution regardless of the easy-axis directions, and it is small when the applied field is close to coercive field, where the magnetization is closer to the easy axis in individual grains. For hard magnets, the calculations from the effective medium theory

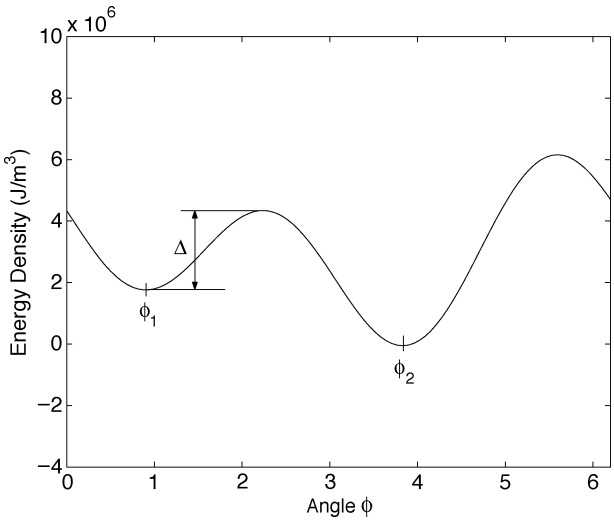

Fig. 6. Energy barrier between metostable state and equilibrium state.

agree with micromagnetic simulation very well, suggesting not only that the magnetization distribution in the material at any applied magnetic field is accurately characterized, but also that our numerical integration is accurate. For the intermediate magnets, the agreement is again less impressive near the coercive field, suggesting that our characterization of magnetization distribution is not very accurate, because we have not considered the subnucleation field switching yet.

IV. Subnucleation Field Switching

While the proposed model represents improvement over Stoner–Wohlfarth model by considering the intergranular magnetostatic interactions using an effective medium approximation, it does not differentiate different grains having identical orientation, which may lead to the deviation of model prediction from actual physical process. In reality, field variation among grains having identical orientation is inevitable, and some grains will switch at an applied field that is smaller than nucleation field. This is especially important when the magnets are not very hard and the energy barrier between metostable state and equilibrium state is relatively small, so that a small variation of magnetic field will provide sufficient energy for some of grains to overcome the energy barrier, resulting switching at subnucleation field. We will account for subnucleation field switching in this section.

With the energy barrier for a grain at orientation θ, $\Delta(\theta)$, determined from our previous analysis (see Fig. 6), we propose that the probability of a grain to overcome the energy barrier and switch at a subnucleation field is

$$p(\theta) = e^{-\frac{\Delta(\theta)}{a\lambda}} \tag{33}$$

where a is a constant to be determined. Recall that λ is a function of J_s^2, and thus is proportional to the magnetic energy in a grain, which provides driving force for the magnetization reversal. Clearly, when the energy barrier is high, such as in hard magnets, the subnucleation field switching rarely occurs; while when the energy barrier is small, such as in soft magnets, the subnucleation field switching will lead to reduced coercivity. At nucleation field where the energy barrier is zero, all the grains at

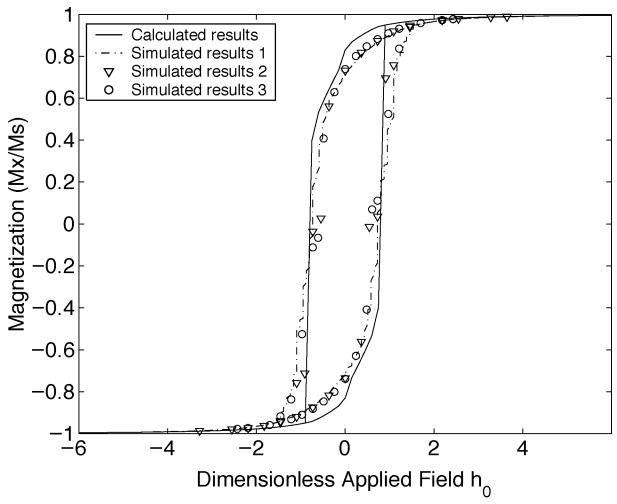

Fig. 7. Hysteresis of a medium magnet ($\lambda = 0.8$) using the probability-based effective medium model.

orientation θ will be switched. With this correction, the average magnetic polarization is determined as

$$f = \int_0^{\pi} [1 - p(\theta)] \cos\phi_1(\theta) w(\theta) d\theta + \int_0^{\pi} p(\theta) \cos\phi_2(\theta) w(\theta) d\theta \tag{34}$$

replacing (23), where ϕ_1 and ϕ_2 are the two stable solutions.

The essence of this correction for subnucleation field switching is that now we differentiate grains at identical orientations into two different groups having different magnetization, thus represents another improvement over the standard effective medium approximation where all grains having same orientation is regarded as identical. As we show in Fig. 7, this correction result in better agreement between effective medium calculation and micromagnetic simulation for intermediate magnet $\lambda = 0.8$, where $a = 0.85$ is used; the same fitting parameter also works well for hard ($\lambda = 0.08$) and other intermediate magnets ($\lambda = 0.5, 1$).

V. Conclusion

We have developed an effective medium theory to calculate the magnetization reversal and hysteresis loop in ferromagnetic polycrystal, where the intergranular magnetostatic interaction is considered. Our calculations using this theory agree with micromagnetic simulations well, and also reveal the importance of subnucleation field switching when the magnet is not very hard.

References

[1] E. C. Stoner and E. P. Wohlfarth, "A mechanism of magnetic hysteresis in heterogeneous alloys," *Phil. Trans. R. Soc. A*, vol. 240, pp. 599–642, 1948.

[2] D. C. Jiles, "Recent advances and future directions in magnetic materials," *Acta Mater.*, vol. 51, pp. 5907–5939, 2003.

[3] E. F. Kneller and R. Hawig, "The exchange-spring magnet: A new material principle for permanent magnets," *IEEE Trans. Magn.*, vol. 27, no. 4, pp. 3588–3600, Jul. 1991.

[4] J. Fidler and T. Schrefl, "Micromagnetic modeling—the current state of art," *J. Phys. D, Appl. Phys*, vol. 33, pp. R135–R156, 2000.

[5] D. L. Atherton and J. R. Beattie, "A mean field Stoner-Wohlfarth hysteresis model," *IEEE Trans. Magn.*, vol. 26, no. 6, pp. 3059–3063, Nov. 1990.

[6] H. L. Qu and J. Y. Li, "Remanence enhancement in magnetically interacting particles," *Phys. Rev. B, Condens. Matter*, vol. 68, no. 212 402, 2003.

[7] D. C. Jiles and D. L. Atherton, "Theory of ferromagnetic hysteresis," *J. Magn. Magn. Mater.*, vol. 61, pp. 48–60, 1986.

[8] J. Y. Li, "Magnetoelectric Green's functions and their application to the inclusion and inhomogeneity problems," *Int. J. Solids Struct.*, vol. 39, pp. 4201–4213, 2002.

[9] J. R. Willis, "Bounds and self-consistent estimates for the overall properties of anisotropic composites," *J. Mech. Phys. Solids*, vol. 25, pp. 185–202, 1977.

[10] T. Schrefl, J. Fidler, and H. Kronmüller, "Remanence and coercivity in isotropic nanocrystalline permanent magnets," *Phys. Rev. B, Condens. Matter*, vol. 49, pp. 6100–6110, 1994.

[11] R. J. Roe, "Description of crystalline orientation in polycrystalline materials, III. General solution to pole figure inversion," *J. Appl. Phys.*, vol. 36, pp. 2024–2031, 1965.

[12] J. Y. Li, "The effective electroelastic moduli of textured piezoelectric polycrystalline aggregates," *J. Mech. Phys. Solids*, vol. 48, pp. 529–552, 2000.

[13] W. H. Press, S. A. Teukolsky, and W. T. Vetterling, *Numerical Recipes in C*. Cambridge, U.K.: Cambridge Univ. Press, 1992.

[14] M. J. Donahue and D. G. Porter, *OOMMF User's Guide, Version 1.0*. Gaithersburg, MD: National Institute of Standards and Technology, 1999.

[15] K. Z. Gao, E. D. Boerner, and H. N. Bertram, "Energy surface model of single particle reversal in sub-Stoner-Wohlfarth switching fields," *J. Appl. Phys.*, vol. 93, pp. 6549–6551, 2003.

Heliang Qu received the B.E. degree in engineering mechanics from Tsinghua University, Beijing, China, in 2002 and the M.S. degree in engineering mechanics from the University of Nebraska-Lincoln in 2004. She is currently working toward the Ph.D. degree as a Graduate Research Assistant in the Department of Engineering Mechanics, University of Nebraska-Lincoln.

Her research focuses on the properties of nanocrystalline ferromagnetic materials, including exchange coupling, magnetostatic interaction, and magnetostriction.

JiangYu Li received the B.E. degree in materials science and engineering from Tsinghua University, Beijing, China, in 1994 and the Ph.D. degree in mechanical engineering from the University of Colorado-Boulder in 1998.

He did three-year postdoctoral studies at the University of California-San Diego and California Institute of Technology afterward. He then joined the Department of Engineering Mechanics at the University of Nebraska-Lincoln as an Assistant Professor in 2001. His current research interest is in the modeling and simulations of ferroelectric and ferromagnetic materials.